Heliyon 9 (2023) e18803

Contents lists available at ScienceDirect

Heliyon

journal homepage: www.cell.com/heliyon

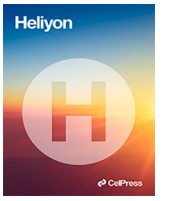

The effect of flexible obstacles with different thicknesses on explosion propagation of premixed methane-air in a confined duct

Zheshi Wang, Zengliang Zhang *, Jia Yu, Zhi Zhai

College of Environmental and Safety Engineering, Qingdao University of Science and Technology, Qingdao, 266000, China

ARTICLE INFO

Keywords:
Methane explosion
Flexible obstacle
Obstacle thickness
Flame behaviour
Overpressure

ABSTRACT

The effect of flexible obstacles with varying thicknesses on the explosion characteristics of combustible gas in a simulated confined duct (cross section 80 mm × 80 mm, length 3 m) was experimentally investigated, aiming to reduce the huge losses caused by gas explosion accidents in the process industries and mining industries. In this paper, plant fiber membranes with an opening area of 0 and thicknesses of 0.105 mm, 0.210 mm, 0.315 mm, 0.420 mm, 0.525 mm, and 0.630 mm were selected as flexible obstacles. The thickness of the flexible obstacle determines the strength of its compressive resistance. The characteristics of overpressure and flame during methane explosions are analyzed and conclusions are drawn. Results indicate that several shock wave reflection processes occur before the diaphragm ruptures, resulting in turbulent flames. In addition, the explosion wave generated numerous shock reflections during the rupture process of the diaphragm, which was gradually discharged downstream of the pipe by ejection as the pressure wave accumulated in front of the diaphragm. It should be noted that the thickness of the flexible obstacle determines the pressure accumulation in front of the membrane. Generally, the thinner the flexible obstacle, the less intense the turbulent flame is induced by the flexible obstacle, decreasing the contact area between the unignited gas downstream of the pipeline and the turbulent flame area. In conclusion, with an increase in the thickness of the flexible barrier, it exhibits a mechanism of initially suppressing and subsequently enhancing the impact on methane explosions. The increase of the thickness of the flexible obstacle motivates the flame propagation speed, which leads to an increase of turbulence intensity and explosion intensity.

1. Introduction

Explosive accidents caused by flammable gas leaks are highly serious in modern industrial and mining industries, and would normally result in a series of consecutive explosions due to a domino effect, resulting in huge economic and property losses and casualties. As a result of a Chinese law entitled “The Fire Protection Law of the People’s Republic of China”, more and more attention is being paid to the matter of combustible gas explosions. There are various types of obstacles in explosion propagation space. Depending on the characteristics of the different obstacles, the obstacles can be divided into rigid and flexible obstacles. These obstacles have an important effect on explosion characteristics. Whether in industrial production, transportation, storage and use, or in coal mining, for safety protection or the needs of work tasks, there are frequently a lot of wind curtains, closed walls, shrubs in the green belt and other flexible objects that can be destroyed. These typical flexible obstacles will promote the formation of turbulence, promote the spread of

* Corresponding author.
E-mail address: 284434231@qq.com (Z. Zhang).

https://doi.org/10.1016/j.heliyon.2023.e18803
Received 27 February 2023; Received in revised form 25 July 2023; Accepted 28 July 2023
Available online 6 August 2023

explosion. Compared with rigid obstacles such as large machinery and equipment, the influence mechanism of these flexible obstacles on combustible gas explosion in confined space is significantly different. The rigidity/flexibility of the obstacle itself is an influential factor affecting the explosion process. Rigid obstacles will not change in BR (Block ratio) during the explosion process, while flexible obstacles will irreversibly deform with the increase of explosion pressure and temperature. Li et al. found that before the reflected wave generated by the flexible/rigid obstacle in the pipeline acts on the flame front, the flame front propagation in the 2 working conditions is similar, and the flame acceleration in the rigid obstacle is more obvious than that in the flexible obstacle [1]. In the current state of research, many researchers are focusing on the impact of rigid obstacles on the explosive properties of combustible gases. The rigid perforated plate obstacle in the pipeline will affect the explosion characteristics of combustible gas, and the explosion intensity will also change with the change of the obstacle position and BR [2,3]. Ciccarelli et al. found that the detonation propagation limit was determined based on the successful transmission of detonation waves from the front half without obstacles to the back half full of obstacles, so the rigid hole plate spacing had a greater impact on the hole plate with high BR and a smaller impact on the hole plate with low BR [4]. The sharper the edge of the rigid obstacle, the more likely it is to induce turbulence, leading to flame acceleration and pressure rise [5,6]. There has been a large and well-studied previous work on rigid obstacles, but the existing work on flexible obstacles is minor.

The thickness of flexible obstacles has a significant influence on the explosion development process. Liu et al. studied the influence of flexible barrier (BOPP film) with thickness of 0.09 mm and 0.1 mm on explosion propagation characteristics, and found that when the thickness of the film increased to 0.1 mm, the peak flame velocity increased by 20.85% [7]. In particular, the presence of a flexible obstacle was found to make the explosive response more violent compared to experiments with a load-free pipe. Wang et al. studied the effects of hydrogen concentration and flexible obstacle thickness on explosion propagation and found that they were positively correlated with explosion intensity [8]. Li et al. found that in the deformation process of the flexible obstacle after the explosion impact, the front of the flame is dominated by the shear layer at the front of the obstacle and the downstream vortex [9]. Ni et al. using OpenFoam software, simplified and simulated the influence of arc-shaped vertical obstacles with different chords in pipeline on explosion characteristics under two-dimensional conditions, and found that the smaller the obstacle, the less likely it is to induce turbulence [10]. Zhang et al. studied two kinds of flexible obstacles with thickness of 0.025 m and 0.425 m when they approached the end of pipeline, and found that the thickness of flexible obstacles had little influence on the explosion characteristics [11]. In actual explosion propagation, the thickness of the obstruction is usually more complex, and when the flexible obstacle is placed at the end of the pipe, its influence on the explosion characteristics cannot be described fully. Therefore, it is necessary to conduct further research on the effect of flexible obstacle thickness on the propagation of explosions. Previous studies have been carried out on the influence of flexible obstacle thickness changes on explosion propagation, but the existing studies have adopted a large range of obstacle thickness changes and fewer working conditions, and additional variables (such as gas concentration, pipeline configuration, etc.) have numerous influencing factors. In actual explosion propagation, the thickness of the obstacle is normally more complex, and its effect on the explosion properties cannot be adequately explained when the flexible obstacle is set at the end of the pipe. Therefore, the mechanism of influence of flexible obstacle thickness variation on explosion propagation needs to be further investigated.

In this paper, a series of methane - air premixed combustible gas explosion experiments were carried out in a closed pipe. The purpose of this paper is to intensively explore the effect of the thickness shift of flexible barriers on the explosive propagation of combustible gases, thus providing a theoretical reference for disaster prevention and mitigation of combustible gas explosions and

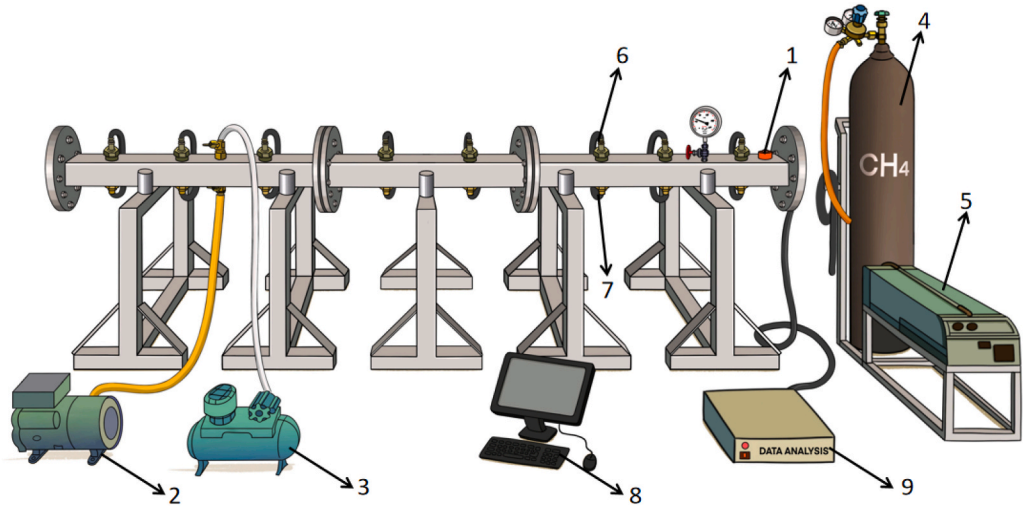

1-ignition system; 2-vacuum pump; 3- air compressor ; 4- methane gas bottle; 5- gas flowmeter; 6-photoelectric sensor; 7-pressure sensor; 8-data analysis computer; 9-data acquisition facility.

Fig. 1. Experimental facility.

safety design in confined spaces.

2. Experimental approaches

Fig. 1 shows the schematic diagram of the experiment. The system consists of a closed explosion pipeline, an ignition system, a methane premix and distribution device, and a dynamic data acquisition device. The explosive duct is composed of three square pipes of 1000 mm in length, with a total length of 3000 mm and a cross-section size of 80 mm × 80 mm. The wall thickness of the tube is 20 mm and the material is 20G high quality carbon structural steel. The maximum bearing pressure can be up to 6.5 MPa, which fully meets the safety requirements of the experiment. The ignition energy of the igniter is 6 J, which is set at 0.1 m from the starting point of the pipeline [12]. The dynamic data acquisition device includes 8 photoelectric sensors radially arranged to record flame intensity and pressure changes in the closed pipe, 8 pressure sensors, data acquisition device and data analysis computer. The range of photoelectric sensor is 0-5v, and that of pressure sensor is 0–1 MPa [13]. Since the sensor cannot directly collect the flame intensity signal, the photoelectric intensity signal is used to characterize the flame. Photoelectric and pressure sensors are arranged on the two walls of the pipe from right to left (distance 0.1 m, 0.3 m, 0.7 m, 1.1 m, 1.3 m, 1.7 m, 2.1 m, 2.7 m from ignition successively).

Fig. 2 presents the schematic diagram of the flexible obstacle (the main components include cellulose, hemicellulose, lignin). Plant fiber film (70 g/m^3) is selected as the material of flexible obstacle. Plant fiber membranes have three characteristics: (1). They have some tear resistance and meet experimental requirements; (2). High safety and low pollution; (3). Access is relatively easy. The area of the obstacles is 120 mm × 120 mm, and their thicknesses are 0.105 mm, 0.210 mm, 0.315 mm, 0.0420 mm, 0.525 mm and 0.630 mm respectively. Their compressive strength is successively increased. When the area of the flexible obstacle is constant, the increase in thickness will lead to an increase in compressive strength. For this reason, the compressive strength of flexible obstacles is determined by using the thickness of these obstacles as a criterion for determining the compressive strength. Usually, the thickness of flexible obstacles serves as a criterion for determining their compressive strength. The opening area of the obstacle is 0, and the loading position is 0.9 m away from the ignition point (as shown in Fig. 3). Table 1 shows thickness, cross section radius and loading position of flexible obstacles under different working conditions. Methane is a typical combustible gas that is not only widely present in nature, but also a widely used gas. Therefore, methane was chosen as the representative combustible gas in this study. In order to highlight the explosive effects of combustible gas and to facilitate the analysis of explosive properties, the equivalent concentration of combustible gas is usually chosen. The equivalent concentration of methane explosion in the air is 9.5%. However, the complete vacuum cannot be achieved in the experimental vacuum extraction process. There is still some air in the pipe, which will reduce the concentration of the gas and thus affect the experimental results. After comprehensive calculations and preliminary experiments, it is known that the explosion intensity of methane gas at 10% concentration is the largest in this experiment. Therefore, 10% methane/air mixture gas was chosen as the experimental gas in this experiment.

The explosion duct, ignition system, gas distribution system, data acquisition system, and exhaust system were assembled together to ensure proper integration of each system. The pipeline's airtightness was tested using a vacuum pump to ensure that the pressure inside the pipeline could be evacuated to below −0.095 MPa, meeting the experimental requirements. Premixed methane gas was prepared with a air compressor and gas flow meter at a concentration of 10%. The concentration of premixed gas filled in the front part of the inner membrane and the back part of the membrane of the pipeline is kept the same, and the premixed gas is left for 30 s to keep stable [14–16]. The ignition system was activated to ignite the combustible mixture inside the pipeline, while simultaneously, the data acquisition system captured the flame signal and pressure signal variations during the explosion process within the duct. At the end of the experiment, the combustion gas was discharged with an air compressor. Each experiment was repeated five times to ensure repeatability.

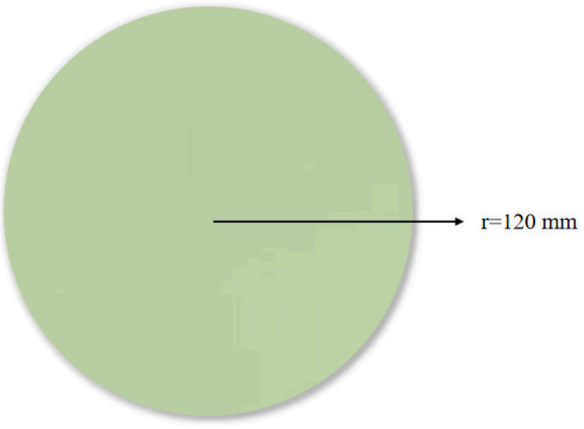

Fig. 2. Plant fiber film.

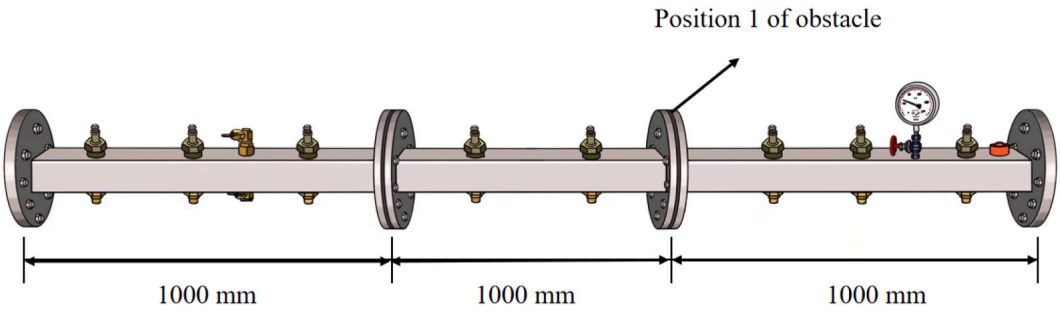

Fig. 3. Obstacles position.

Table 1
Details of flexible obstacles used in this study, including the thickness (mm).

Working condition	Radius (mm)	Thickness (mm)	Loading position
C_1	120	0.105	Position 1
C_2	120	0.210	Position 1
C_3	120	0.315	Position 1
C_4	120	0.420	Position 1
C_5	120	0.525	Position 1
C_6	120	0.630	Position 1

3. Results and discussion

In this paper, the effect of flexible obstacles with different thicknesses on methane explosion in a confined duct is studied. On this basis, the overpressure characteristics, flame velocity and flame intensity of the explosion process under the conditions of flexible

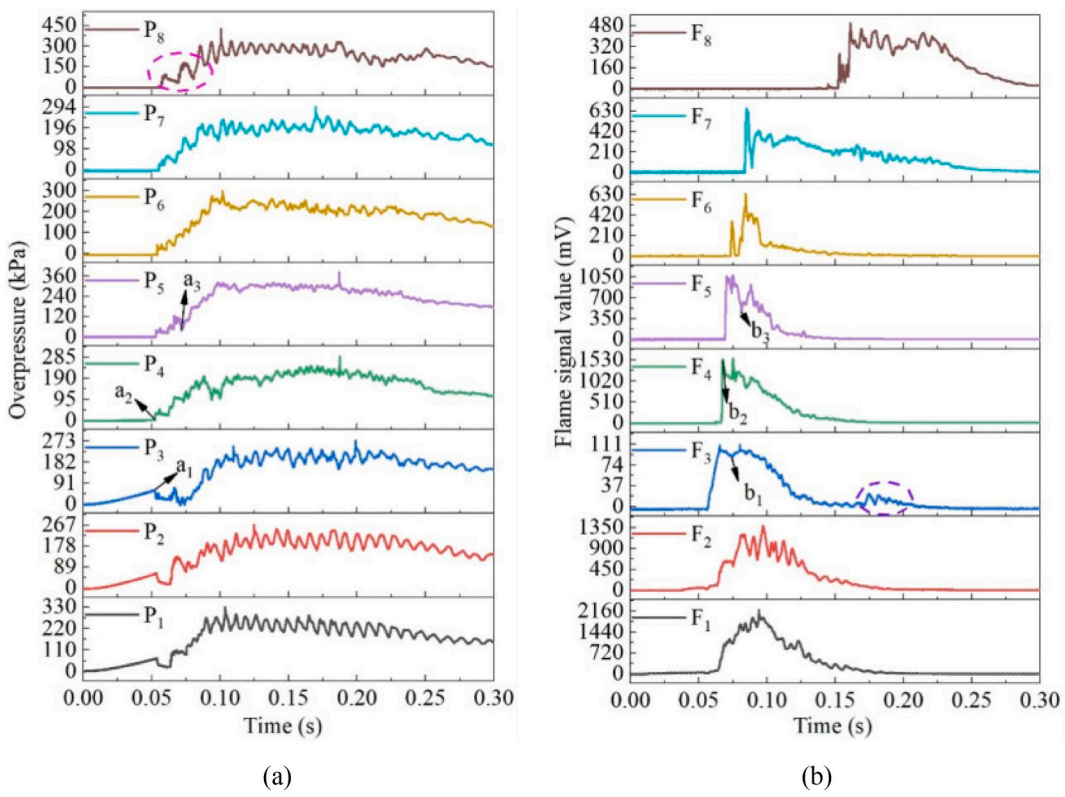

Fig. 4. The overpressure-time histories (a) and flame intensity-time histories (b) of the experiment with flexible obstacle with a thickness of 0.105 mm.

obstacles with different thicknesses in a closed duct are analyzed. In addition, the effect of the end blind plate on methane explosion in a closed pipeline is analyzed.

Since the flame intensity and overpressure change trend of the flexible obstacle experiment with different thickness are basically the same, the flexible obstacle experiment with thickness of 0.105 mm is taken as the representative for the overall analysis. Fig. 4 shows the overpressure-time profiles [Fig. 4(a)] and flame intensive-time profiles [Fig. 4(b)] of the experiment for a flexible obstacle with a thickness of 0.105 mm. The analysis is performed in combination with the peculiar changing processes of the membrane during the explosion, as shown in Fig. 5. Explosion of premixed methane and air in the pipeline can be divided into three stages. The first stage is the propagation of the explosion before the membrane breaks. After the igniter ignites, the generated electric spark ignites the combustible gas near the electrode. The flame front formed by the combustion of combustible gas develops at the front of the explosion. The unignited gas driven by the expansion wave accumulates upstream of the flexible obstacle, leading to a stable rise in the upstream overpressure of the flexible obstacle (before points a_1 and b_1). With the shortening of the distance between the explosion flame and the flexible obstacle, the accumulation of a large amount of unburned gas and the impact of pressure wave in the upstream of the film make the flexible obstacle fixed by screws to conical deformation in the direction of explosion propagation. There are two reasons for this phenomenon. On the one hand, the geometric center position of the obstacle has the lowest binding force and is freer than the other positions due to the tight binding effect of the bolts around the obstacle. On the other hand, the closer the distance to the wall, the stronger the attraction due to the attraction effect of the pipe wall. The intensity of the precursor shock wave is the highest at the center of the cross section, and the propagation speed of the flame front is the fastest at the center of the cross section. As a result, the obstacle is subjected to the pressure of the vertical arc plane towards the direction of explosion, and the closer it is to the geometric center of the obstacle, the greater the resultant force, thus making the obstacle undergo conical deformation.

The second stage is the propagation of the explosion during membrane rupture. When the explosion flame propagates to about 0.4 m away from the ignition point, part of the mixed gas accumulated in front of the film will take the weak link of the flexible obstacle as the breakthrough point and spray to the direction behind the film (before points a_2 and b_2). The high-pressure area near the front of the membrane instantly becomes the low-pressure area, forming a pressure difference with the high-pressure area near the front of the flame, resulting in a downward trend of the upstream overpressure of the flexible obstacle overall. It is important to note that the shock oscillations formed during this phase and the effect of the jet on the downstream gas field of the film will induce the formation of turbulence, leading to the apparent high frequency fluctuations in the upper and lower part of the pressure excess curve.

The third stage is the propagation of the explosion after the membrane is completely removed. Laminar flame gradually develops into turbulent flame, forming three-dimensional combustion. As the flame front gets closer and closer to the end blind plate, the flame intensity decreases due to the reflected wave caused by the barrier effect of the blind plate (after points a_3 and b_3). At the same time, a large amount of unburned gas accumulated in the end-blind plate is pushed towards the front of the flame by the reflected wave. After a short induction period, it is added to the burning reaction in the turbulent region, stabilizing the excess pressure at a relatively elevated level overall. Under specific thickness, tempering will occur (as shown in the purple box of F_3 in Fig. 6). At the same time, a large amount of unburned gas accumulated in the end blind plate is pushed towards the front of the flame by the reflected wave. After a short induction period, it is added into the combustion reaction in the turbulent region, making the overpressure stable at a relatively elevated level on the whole. Under specific thickness, tempering will occur (as shown in the purple box of F_3 in Fig. 6). It is worth noting that after three-dimensional combustion is formed in the pipeline, on the one hand, the high-intensity shock wave will promote the flame combustion, so that the flame forms a local “bright” area; on the other hand, it also quenches the flame, causing the flame to form local “dark” areas, resulting in a wide range of flame signal changes. Finally, with the constant consumption of combustible gas, the flame gradually extinguishes (as shown in Fig. 6). In the process of flame propagation, the time for expansion wave generated by explosion to break through the flexible obstacle in the experiment of flexible obstacle with thickness of C_6 (hereinafter uniformly

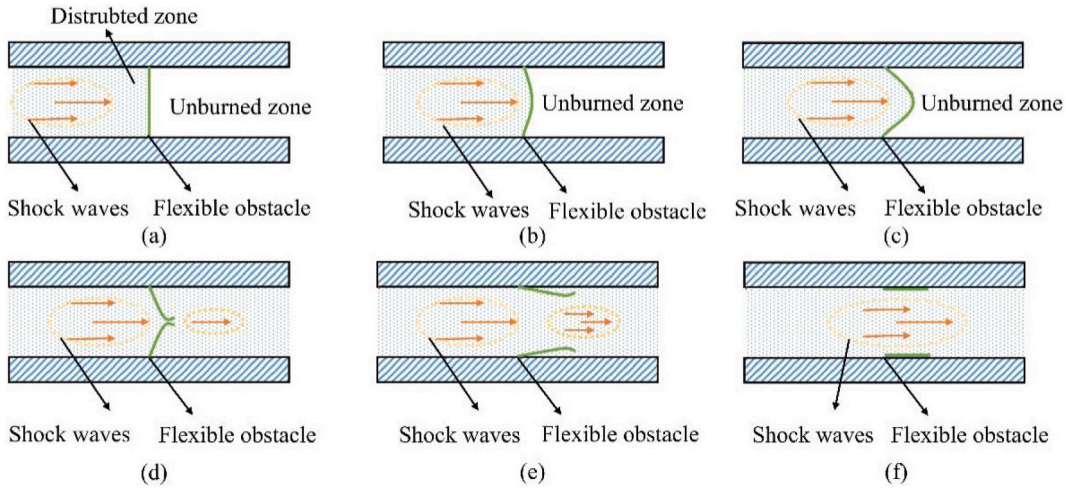

Fig. 5. Diagram of the film breaking process during an explosion in a pipe.

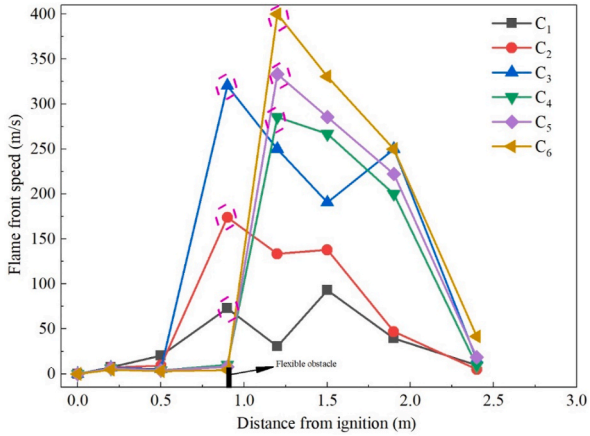

Fig. 6. Flame front speed profiles in duct.

referred to as film breaking time) is greater than the experimental results of other flexible obstacles with thickness of C_1 in particular. This is because the pressure strength of the flexible obstacle increases with the increase of the thickness of the flexible obstacle, and the stability of the jet flow decreases with the increase of the thickness of the flexible obstacle. As a result, the turbulence strength downstream of the flexible obstacle increases with the increase of the thickness of the flexible obstacle (as shown in Fig. 7).

Fig. 6 shows the velocity profiles of the flame front in the experimental duct under the conditions of flexible obstacles with different thicknesses. In the process of explosion propagation, before the flexible obstacle is broken through by an expansion wave, the flame velocity of each experiment is basically the same. In addition, the acceleration of flame propagation is relatively low under the influence of pressure waves reflected from the obstacle [17]. As the distance from the flexible obstacle shortened, the influence of the reflected pressure waves continued to increase, and the flame propagation velocity gradually decreased. After 0.24 m away from the ignition source, the flame propagation speed is accelerated under the influence of the excitation effect produced by membrane rupture. Based on the results of the analysis, it can be concluded that there is a low intensity of the reflected pressure wave at the corresponding position of the flexible obstacle. As the pressure wave gradually breaches the flexible obstacle, the excitation effect of the pressure difference between the front and back of the membrane is greater than the inhibition effect of the reflected wave. In addition, the flow of gas in front of the membrane accelerates the airflow around the membrane, which is conducive to the propagation of the flame. The gas ejected from the weak link of the flexible obstacle has a high velocity. Under its influence, the flame velocity increases greatly after the explosion passes through the flexible obstacle. In response to an increase in the thickness of a flexible obstacle, the pressure that accumulates in front of the film increases. At a distance of 1.3 m from the ignition point, the flame front velocity in the experiment with a flexible obstacle of thickness C_6 is significantly higher than the velocity in the experiment with a smaller flexible obstacle.

As the flame propagates, the time it takes the expansion wave generated by the explosion to crack through the flexible obstacle (hereinafter referred to as the film breaking time) is larger than the experimental results of the flexible obstacle with other thicknesses (especially the flexible obstacle with thickness C_1). In this case, the bearing strength of the flexible obstacle increases as its thickness

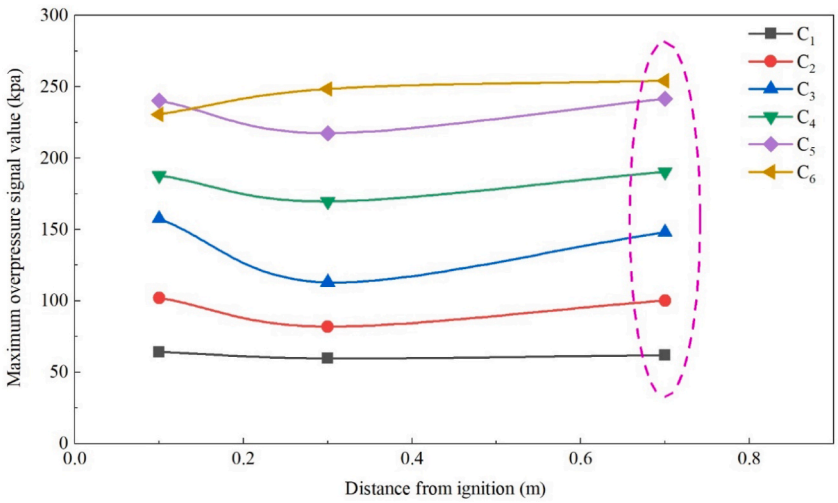

Fig. 7. Maximum overpressure profiles of explosion before membrane rupture.

increases, while the stability of the jet flow decreases as the thickness of the flexible obstacle increases, causing an increase in turbulence downstream of the flexible obstacle as a result [18–20]. When the thickness of the flexible obstacle is smaller, turbulent flame formation occurs earlier, but the turbulence intensity is weaker. Therefore, the flame propagation acceleration of the flexible obstacle with thickness C_6 is greater than that of other flexible obstacles. The thickness changes of the six closed flexible obstacles are obvious (the thickness of the C_6 flexible obstacle is 6 times that of the C_1 flexible obstacle), but in the third stage of the explosion process, the flame velocity of the 6 groups of experiments is basically the same. It is evident that the increase in the thickness of the flexible obstacle does not have an obvious effect on the excitation of the flame front propagation velocity downstream of the explosion.

Fig. 7 shows the maximum overpressure profiles of the explosion in the pipeline before membrane rupture. The flexible obstacle causes a barrier effect, so only the upstream pressure sensor can collect the pressure signal before the barrier is breached. It can be found that as the flame approaches the flexible obstacle, the maximum overpressure first falls and then increases. Combined with the above analysis, when the explosion propagates to 0.3 m near the fire source of the stronghold, the reflected wave generated by the flexible obstacle acts on the explosion shock wave area. The resistance to explosion propagation increases gradually, and the pressure accumulated in front of the membrane increases gradually. At 0.7 m away from the ignition point, the peak overpressure of the 6 groups of experiments is C_1, C_2, C_3, C_4, C_5, C_6 from small to large. However, at 0.1 m away from the ignition point, the peak overpressure value in C_6 working condition is lower than that in C_5 working condition, which is a serious peak overpressure. This is because with the increase in the thickness of the flexible obstacle, the inhibitory effect of the reflected wave generated by the barrier effect of the flexible obstacle on the explosion wave is enhanced.

Fig. 8 shows the maximum overpressure profiles of the explosion in the pipeline after membrane rupture. The peak overpressure in the pipeline is the result of the explosion during membrane rupture and the explosion after membrane rupture. The pressure wave generated in the turbulent flame area and the pressure wave reflected from the front blind plate are superimposed, and the explosive airflow accumulates in front of the blind plate, resulting in a very high overpressure value at 0.1 m from the ignition point. In the process of membrane breaking, the inhibitory effect of flexible obstacles on explosion gradually decreases, and the excitation effect gradually increases. It is clear from comparing the profiles of maximum overpressure after membrane rupture with that before membrane rupture that the overall influence of the breaching process of the flexible obstacle on the peak overpressure is the incentive effect. The explosion developed quickly after breaking through the flexible obstacle. After the flexible obstacle is completely breached by the explosion wave, the creased flame front quickly ignites the unignited gas, and the explosion propagates from the center of the pipeline to the wall, resulting in the peak overpressure at 1.3 m away from the ignition point being greater than that at 1.1 m away from the ignition point. At 1.7 m away from the ignition point, the reflected wave generated by the terminal blind plate acts on the explosion wave, which has a certain inhibitory effect on the explosion. With the development of the explosion, a large amount of unignitable gas accumulated in the terminal blind plate moves to the front of the flame, driven by the reflected wave, and adds to the flame combustion, increasing the overpressure. At 2.8 m away from the ignition, the peak overpressure of the 6 groups of experiments from small to large is C_1, C_2, C_3, C_4, C_5, C_6. In accordance with the results of the analysis, the overpressure downstream of the flexible obstacle is primarily affected by the intensity of turbulence and the intensity of explosions. When the film is broken, the greater the pressure of explosion spraying behind the film, the easier it is to make the flame fold increase, leading to the increase of explosion intensity [21]. Although the increase in the thickness of the flexible obstacle prolongs the film breaking time, it also increases the amount of turbulent flow induced by pressure drop. In addition, the greater the turbulence intensity induced by the flexible obstacle, the more fully the large amount of unignited gas near the terminal blind plate can participate in the turbulent combustion reaction. The thickness of C_1–C_6 flexible obstacles increases in turn, resulting in stronger peak overpressure due to its special excitation effect on the explosion process. This further illustrates the risk of combustible gas explosion with the increase of flexible obstacle thickness.

The flame signal data collected by each photodetector on the pipe has only a single peak and the flame signal curve fluctuates regularly. Therefore, the maximum flame signal data is used as a proxy to analyze the explosion propagation process (as shown in Fig. 9). In the process of flame propagation, because of the excitation effect of the flexible porous obstacle, the flame signal value of the obstacle loaded with flexible pores is clearly higher than that of the no-load arrangement. The jet generated during the film breaking process agitates the gas field downstream of the film, making the flame front contact with the combustible gas in the unburned area more completely, resulting in the flame gradually developing into turbulence, and the maximum value of the excited flame signal starts to decrease at 0.3 m, forming the first peak value. Then the flame signal value develops again. The peak intensity of the flame signal around 1.3 m gradually decreases due to the blocking effect of reflected waves generated by the end blind plate and the consumption of combustible gas. However, as the large amount of unburned gas accumulated at the end blind plate moves in the opposite direction to the flame front due to the compression of the expanding wave, it rejoins the explosion reaction and forms a second peak near the end blind plate.

The trend of the variation of the values of the peak flame signal is similar for flexible pore obstacles with different pore areas. Conversely, the tempering in the C_6 condition is weak and does not spread to the near end of the pipe. For flexible obstacle thicknesses C_1–C_3, the intensity of the first peak flame signal increases with increasing obstacle thickness. When the obstacle thickness exceeds C_4, the intensity of the first peak flame signal decreases as the obstacle thickness increases. In particular, after the turbulent flame region is formed under various working conditions, the intensity of shock wave further generated by explosion is also inconsistent due to different turbulence intensity and unequal amount of combustible gas consumed, leading to the difference in the intensity variation amplitude of the second peak flame signal. It should be noted that the intensity of turbulence formed during the overall explosion is strongest in the C_3 condition. The turbulent intensities formed during the explosions of C_1 and C_6 are relatively low.

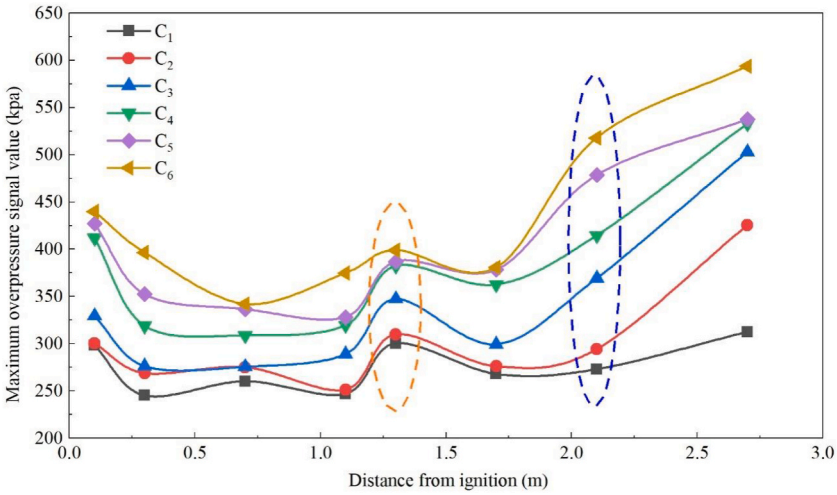

Fig. 8. Maximum overpressure profiles of explosion after membrane rupture.

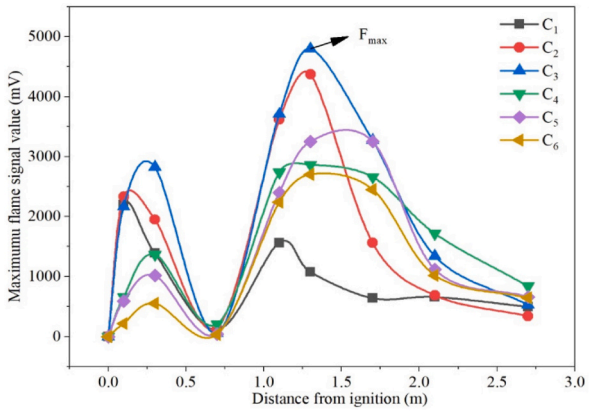

Fig. 9. Peak flame signal value profiles in duct.

4. Conclusion

In this paper, premixed methane - air detonation experiments were carried out in a 3 m long confined duct. Flexible obstacles with thickness of 0.105 mm, 0.210 mm, 0.315 mm, 0.0420 mm, 0.525 mm and 0.630 mm were loaded into the pipeline to determine their influence on the explosion propagation. The thickness of the flexible obstacle is taken as the standard to judge the bearing strength of the flexible obstacle. The main conclusions are as follows:

(1) When the flexible obstacle is not breached by the explosion, the increase of the thickness leads to the increase of the ability to inhibit the explosion development.
(2) The increase of the thickness of the flexible obstacle prolongs the time of exploding film. However, when the thickness of the flexible obstacle reaches a certain value, the effect is not obvious.
(3) When the explosion breaks through the flexible obstacle, under the action of airflow and the pressure difference between the front and rear regions of the membrane, the explosion will have obvious excitation effect. The thickness is positively correlated with the peak overpressure downstream of the flexible obstacle. Reducing the peak overpressure during explosion is of great significance to safety design.
(4) The overpressure downstream of the flexible obstacle is mainly caused by turbulence and explosion intensity. The increase of the thickness of the flexible obstacle leads to the increase of the turbulence downstream of the flexible obstacle, which leads to the increase of the peak overpressure.
(5) When the obstacle is set upstream of the pipe, the intensity of the peak flame signal increases with increasing obstacle thickness when the thickness of the flexible obstacle is less than 0.315 mm. When the obstacle thickness exceeds 0.315 mm, the intensity of the peak flame signal decreases with increasing obstacle thickness.

Author contribution statement

Zheshi Wang: Conceived and designed the experiments; Performed the experiments; Analyzed and interpreted the data; Contributed reagents, materials, analysis tools or data; Wrote the paper.

Zengliang Zhang, Ph.D: Conceived and designed the experiments; Analyzed and interpreted the data; Contributed reagents, materials, analysis tools or data; Wrote the paper.

Jia Yu, Zhi Zhai: Performed the experiments.

Data availability statement

Data will be made available on request.

Declaration of competing interest

The authors declare that they have no known competing financial interests or personal relationships that could have appeared to influence the work reported in this paper.

Acknowledgements

This research did not receive any specific grant from funding agencies in the public, commercial, or not-for-profit sectors.

References

[1] Q. Li, S.X. Lu, M.J. Xu, Y.M. Ding, C.J. Wang, Comparison of flame propagation in a tube with a flexible/rigid obstacle, J. Energy Fuels 30 (10) (2016) 8720–8726, https://doi.org/10.1021/acs.energyfuels.6b01594.

[2] Q.Q. Zuo, Z.R. Wang, Y.Y. Zhen, S.F. Zhang, Y.Q. Cui, J.C. Jiang, The effect of an obstacle on methane-air explosions in a spherical vessel connected to a pipeline, J. Process Saf. Progress. 36 (1) (2017) 67–73, https://doi.org/10.1002/prs.11823.

[3] Z.M. Luo, X.F. Kang, T. Wang, B. Su, F.M. Cheng, J. Deng, Effects of an obstacle on the deflagration behavior of premixed liquified petroleum gas-air mixtures in a closed duct, J. Energy. 234 (2021), https://doi.org/10.1016/j.energy.2021.121291.

[4] G. Ciccarelli, Z. Wang, J. Lu, M. Cross, Effect of orifice plate spacing on detonation propagation, J. Loss Prevent. Process Indust. 49 (2017) 739–744, https://doi.org/10.1016/j.jlp.2017.03.014.

[5] H.K. Byun, D.J. Kim, D.J. Park, Effect of different obstacle geometries on deflagration explosion in a vented chamber, J. Sci. Technol. Energet. Mater. 79 (03–04) (2018) 93–96. https://www.webofscience.com/wos/woscc/full-record/WOS:000447484200006.

[6] L. Wang, R.J. Si, R.Z. Li, Y. Huo, Experimental investigation of the propagation of deflagration flames in a horizontal underground channel containing obstacles, J. Tunnell. Underground Space Technol. 78 (2018) 201–214, https://doi.org/10.1016/j.tust.2018.04.027.

[7] S.S. Liu, J.D. Xu, Y.V. Zhang, et al., Experimental study on influence of flexible obstacle thickness on methane explosion excitation effect, J. Coal Technol. 41 (1) (2022) 106–110, https://doi.org/10.13301/j.cnki.ct.2022.01.024.

[8] X. Wang, C.J. Wang, X.J. Fan, F.P. Guo, Z. Zhang, Effects of hydrogen concentration and film thickness on the vented explosion in a small obstructed rectangular container, J. Int. J. Hydrogen Energy 44 (40) (2019) 22752–22759, https://doi.org/10.1016/j.ijhydene.2018.12.207.

[9] Q. Li, G. Ciccarelli, X.X. Sun, S.X. Lu, X. Wang, Z. Zhang, M.J. Xu, C.J. Wang, Flame propagation across a flexible obstacle in a square cross-section channel, J. Int. J. Hydrogen Energy 43 (36) (2018) 17480–17491, https://doi.org/10.1016/j.ijhydene.2018.07.077.

[10] J. Ni, J.F. Pan, E.K. Quaye, k. Evans, Numerical simulation of hydrogen-air flame acceleration and detonation initiation in tubes equipped with arc obstacles of different chord lengths, J. Acta Astronaut. 177 (2020) 192–201, https://doi.org/10.1016/j.actaastro.2020.07.025.

[11] S. Zhang, Z.S. Tang, J.L. Li, J.G. Wang, J.Q. Zhang, J. Guo, Q. Li, Effects of equivalence ratio, thickness of rupture membrane and vent area on vented hydrogen–air deflagrations in an end-vented duct with an obstacle, J. Int. J. Hydrogen Energy 44 (47) (2019) 26100–26108, https://doi.org/10.1016/j.ijhydene.2019.08.057.

[12] Z.L. Zhang, H.P. Wang, Z. Wang, W. Tian, Z.S. Wang, The effect of orifice plates with different shapes on explosion propagation of premixed methane–air in a semi-confined pipeline, J. Loss Prevent. Process Indust. 71 (2021) 104498–104503, https://doi.org/10.1016/j.jlp.2021.104498.

[13] Z. Wang, Z.L. Zhang, W. Tian, Z.S. Wang, Coupling effect of side explosion vent and wire mesh on suppressing methane explosion in a closed duct, J. Loss Prevent. Process Indust. 76 (2022), https://doi.org/10.1016/j.jlp.2022.104738.

[14] K. Yang, Q.R. Hu, S.H. Sun, P.F. Lv, L. Pang, Research progress on multi-overpressure peak structures of vented gas explosions in confined spaces, J. Loss Prevent. Process Indust. 62 (2019), 103969, https://doi.org/10.1016/j.jlp.2019.103969.

[15] S.X. Han, M.G. Yu, X.F. Yang, X.Y. Wang, Effects of obstacle position and hydrogen volume fraction on premixed syngas-air flame acceleration, J. Int. J Hydrogen Energy 45 (53) (2020) 29518–29532, https://doi.org/10.1016/j.ijhydene.2020.07.189.

[16] C.Y. Huang, X.F. Chen, L.J. Liu, H.M. Zhang, B.H. Yuan, Yi Li, The influence of opening shape of obstacles on explosion characteristics of premixed methane-air with concentration gradients, J. Process Saf. Environ. Protect. 150 (2021) 305–313, https://doi.org/10.1016/j.psep.2021.04.028.

[17] Z.L. Qiao, H. Ma, Effect of small-size space porous flexible PVC material on propane deflagration, J. AIP Adv. 12 (1) (2022), https://doi.org/10.1063/5.0080201.

[18] X.P. Wen, Z.D. Guo, F.H. Wang, R.X. Pan, Z.C. Liu, X.M. Zhang, Experimental study on the quenching process of methane/air deflagration flame with porous media, J. J. Loss Prevent. Process Indust. 65 (2020), https://doi.org/10.1016/j.jlp.2020.104121.

[19] X.P. Wen, M.M. Wang, F.H. Wang, M.G. Yu, H.X. Deng, Combined effects of obstacle and fine water mist on gas explosion characteristics, J. Chin. J. Chem. Eng. 40 (2021) 131–140, https://doi.org/10.1016/j.cjche.2020.10.042.

[20] J. Wang, Z.Y. Fan, y. Wu, L.G. Zheng, R.K. Pan, Y. Wang, Effects of abrupt changes in the cross sectional area of a pipe on flame propagation characteristics of CH_4/air mixtures, J. ACS Omega. 6 (23) (2021) 15126–15135, https://doi.org/10.1021/acsomega.1c01350.

[21] K. Gao, S.N. Li, Y.J. Liu, J.Z. Jia, X.Q. Wang, Effect of flexible obstacles on gas explosion characteristic in underground coal mine, J. Process Saf. Environ. Protect. 149 (2021) 362–369, https://doi.org/10.1016/j.psep.2020.11.004.